

Article

# The Enzyme-Like Property and Photocatalytic Effect on $\alpha$ , $\alpha$ -Diphenyl- $\beta$ -Picrylhydrazyl (DPPH) of CuPt Nanocomposite

Tao Wen <sup>†</sup>, Doudou Yan <sup>†</sup>, Jie Meng, Jian Liu and Haiyan Xu <sup>\*</sup>

Institute of Basic Medical Sciences, Chinese Academy of Medical Sciences & Peking Union Medical College, Beijing 100005, China; went@ibms.pumc.edu.cn (T.W.); cpuyandoudou@126.com (D.Y.); mengjie@ibms.pumc.edu.cn (J.M.); liujian@ibms.pumc.edu.cn (J.L.)

<sup>\*</sup> Correspondence: xuhy@pumc.edu.cn

<sup>†</sup> These authors contributed equally to this work.

Received: 31 August 2019; Accepted: 26 September 2019; Published: 27 September 2019



**Abstract:** With co-reduction method, a new nanocomposite consisting of Cu and Pt (CuPt) was prepared in household. The morphology of CuPt alloy was characterized by scanning electron microscope (SEM) and transmission electron microscope (TEM). The diameter of CuPt was ca. 125 nm measured by dynamic light scattering (DLS). The atom ratio of Cu to Pt was determined to be about 1.2 by energy-dispersive X-ray (EDX). Enzyme-like activities of CuPt, including peroxidase (POD)-like and ascorbic acid oxidase (AAO)-like activities were examined with UV-Vis-NIR spectrometer. The CuPt was found to interact with  $\alpha$ ,  $\alpha$ -diphenyl- $\beta$ -picrylhydrazyl (DPPH) in the presence or absence of AA. With irradiation by light emitting diode (LED) light, the photocatalysis effect of CuPt on DPPH was investigated. With the addition of histidine, it was proved that singlet oxygen had an important role in the interaction involving CuPt. The new nanocomposite and the properties suggest various potentials of application.

**Keywords:** CuPt; peroxidase (POD)-like; ascorbic acid oxidase (AAO)-like; DPPH

## 1. Introduction

In recent years, certain achievements have been made in the metal nanomaterials as heterogeneous catalysts, and this has led to various applications [1]. Among them, the enzyme-like activity and antioxidant activities of metal nanomaterials have attracted intensive research interests in recent years. To date, nanomaterials such as ferromagnetic nanoparticles, FeS, CuS, ZnS, and noble metals have been reported to hold peroxidase (POD)-like, oxidase-like, catalase-like, superoxide dismutase (SOD)-like, or ascorbic acid oxidase (AAO)-like properties [2,3], and have shown promising potentials in several medical and biological detection systems [4]. Due to the economic cost, controlled synthesis, tunable catalytic activities, and high stability, nanoparticles have been regarded as good candidates as enzyme mimetics.

The nanocomposite consisting of Cu and Pt (CuPt) is a new kind of nanostructure, which was expected to own excellent properties of both metals. Nanoparticles containing Cu and Pt element have been used in various applications: Cu-Pt nanocrystals for CO<sub>2</sub> electroreduction reaction [5] bimetallic core-shell Cu@Pt nanoparticles for antibacterial activity [6], and Pt-Cu bimetallic alloy nanoparticles supported on anatase TiO<sub>2</sub> for photocatalytic aerobic oxidation [7]. As we know, the morphology of metal nanoparticles is the key to exploring the active sites of catalysts and holds great promise for the optimization of them [8]. Several groups have reported porous PtCu dendrites [9], CuO/Pt nanoflowers [10], and PtCu diamond nanoparticle [11] exhibiting enzyme-like activity and

being employed for detection, however, little is known about the nanoparticle involving the same elements (Cu and Pt) with sphere morphology, and their enzyme-like properties and the interactions with antioxidants in applications have been rarely investigated.

In this study, CuPt was synthesized by a co-reduced method and demonstrated to have both POD-like activity and AAO-like activity, evidenced by the characteristic extinction of POD substrate and AA. In addition, the scavenging effect of CuPt on DPPH and their photocatalytic effects were examined, and underlying mechanisms were investigated.

## 2. Results and Discussion

### 2.1. Characterizations of the Nanocomposite Consisting of Cu and Pt

As shown in the image of scanning electron microscope (SEM) (Figure 1A), the prepared nanocomposite was spherical with a rough surface. It can be seen from the image of transmission electron microscope (TEM) that the nanoparticles' diameter is about 125 nm (Figure 1B), consistent with that obtained from the dynamic light scattering (DLS) of  $124.9 \pm 3.7$  nm. The photo of CuPt solution showed black (Figure 1C), that was possibly due to the full wavelength absorption on light (Figure S1). Both Cu and Pt atoms were examined in energy-dispersive X-ray (EDX) detection, and the atom ratio of Cu to Pt was 1.2 (Figure 1D). A powder X-ray diffraction (XRD) pattern of the CuPt displayed peaks between single Cu (JCPDS 04-0836) and Pt (JCPDS 04-0802) (Figure 1E) [12,13], showing that the spherical CuPt was an alloy involving Cu and Pt.

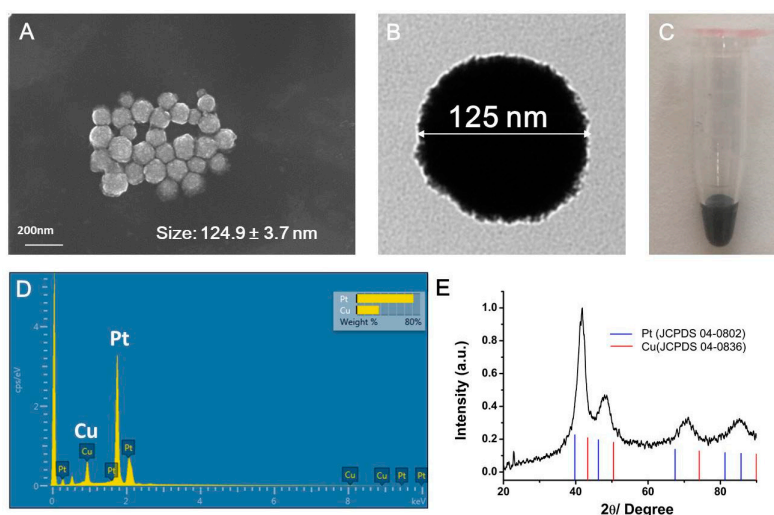


**Figure 1.** Characterizations of the nanocomposite consisting of Cu and Pt (CuPt). (A) Scanning Electron Microscope (SEM) image of CuPt, (B) Transmission electron microscope (TEM) image. (C) Photo of CuPt solution. (D) Energy-dispersive X-ray (EDX) images for CuPt. (E) Powder X-ray diffraction (XRD) pattern of CuPt.

### 2.2. Peroxidase (POD)-Like Activity of CuPt

It has been reported that platinum (Pt) based or copper (Cu) based nanoparticles have excellent enzyme-like characteristics [14]. Therefore, we next examined whether CuPt had enzyme-like activity. Following the protocol for the catalytic activity of peroxidase (POD) evaluation [15], the colorimetric substrate o-phenylenediamine (OPD) in the presence of  $H_2O_2$  was employed. Due to the fact that 2,3-diaminophenazine has an extinction peak at 450 nm, which is produced by POD-catalyzed oxidation of OPD in the presence of hydrogen peroxide [16], we investigated the change of extinction at 450 nm to determine the oxidation degree of OPD. In the neutral phosphate buffer saline (PBS) solution, the addition of CuPt made the solution color change to yellow, while the solution without CuPt was still colorless (Figure 2A). This colorimetric reaction indicated the POD-like activity of CuPt. The POD-like

activity of CuPt in PBS with different pHs was also investigated (Figure S2), showing that the extinction at 450 nm changed larger in the solution of pH 3.65 than that in the neutral and alkaline PBS solutions (Figure 2B). Furthermore, the effects of different concentrations of CuPt were monitored at pH 3.65 (Figure S3). The extinctions at 450 nm were changed in a dose-dependent manner with time in the presence of CuPt (Figure 2C,D).

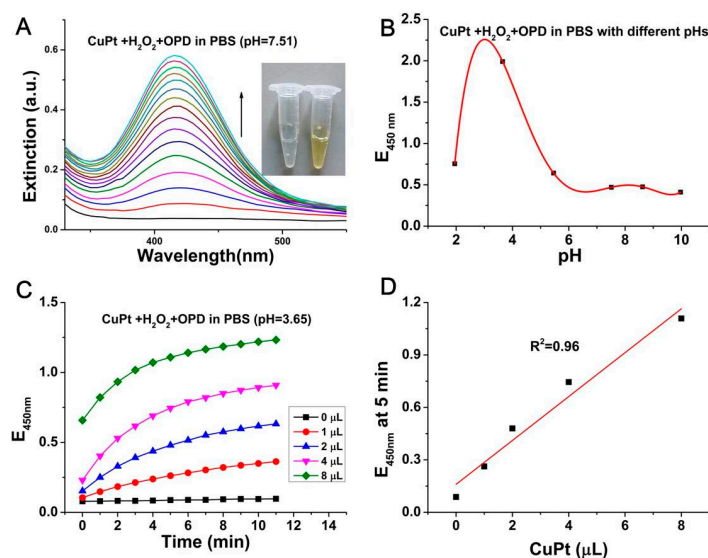


**Figure 2.** Peroxidase (POD)-like activity of CuPt in phosphate buffer saline (PBS). (A) Ultraviolet-visible-near infrared (UV-Vis-NIR) spectra of 1  $\mu\text{L}$  CuPt with o-phenylenediamine (OPD) and  $\text{H}_2\text{O}_2$  in PBS (pH = 7.51) for every 2 min. The insert shows the photograph of corresponding systems in the absence (left) and presence (right) of CuPt. (B) Effect of pH on POD-like activity of 1  $\mu\text{L}$  CuPt in PBS with different pH. (C) Effect of CuPt concentration in PBS (pH 3.65). (D) The concentration-dependent absorbance changes after incubation for 5 min in PBS (pH 3.65). The solutions contain 4.60 mM OPD and 0.50 M  $\text{H}_2\text{O}_2$  for (A), (B), (C) and (D).

The POD-like activity was detected in water as well (Figure 3). As shown in the UV-Vis-NIR spectra of OPD, the extinction at 450 nm in the presence of CuPt (Figure 3B) increased more than that in the absence of CuPt (Figure 3A) within the same time period. Similarly, with the real enzyme horseradish peroxidase (HRP), the extinction at 450 nm of OPD changed (Figure 3C), proving the POD-like activity of CuPt. The extinction change was related to the concentration of  $\text{H}_2\text{O}_2$  in the solution (Figure 3D). With exponential fitting the curve of extinction was at 450 nm vs. various  $\text{H}_2\text{O}_2$  concentrations ( $R^2 = 0.995$ ), suggesting that the POD-like activity of CuPt could be used to detect  $\text{H}_2\text{O}_2$  level.

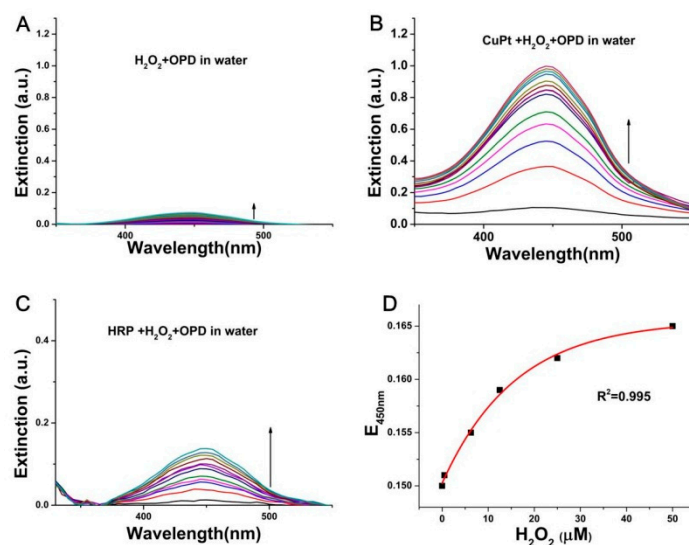


**Figure 3.** Peroxidase (POD)-like activity of CuPt in water and its application in detection of H<sub>2</sub>O<sub>2</sub> concentrations. The time-dependent changes of UV-Vis-NIR spectra with (A) or without (B) the addition of CuPt measured by every 2 min. UV-Vis-NIR spectra were collected in water containing 4.60 mM OPD and 0.50 M H<sub>2</sub>O<sub>2</sub> for 30 min. (C) UV-Vis-NIR spectra of horseradish peroxidase (HRP) oxidize OPD in the presence of H<sub>2</sub>O<sub>2</sub> for every 1 min. [HRP] = 2.3 nM, [OPD] = 4.60 mM, and [H<sub>2</sub>O<sub>2</sub>] = 0.50 M. (D) Dependence of the extinction at 450 nm on different concentrations of H<sub>2</sub>O<sub>2</sub> in water with 1 μL CuPt and 4.60 mM OPD after incubation for 10 min.

### 2.3. Effect of CuPt on AA

As an active reducing agent, ascorbic acid (AA) can be oxidized by oxygen slowly. Optical analysis methods for AA oxidation have attracted considerable attention as the optical analysis holds the features of low cost, rapidity, simplicity and realization of color discrimination. Herein, the effect of CuPt on AA oxidation was investigated by UV-Vis-NIR spectroscopy. It was found that the extinction at 260 nm (characteristic absorption peak for AA) had leveled off after the initial ramp-down with time (Figure 4A) in dose-dependent manner with CuPt (Figure 4B and Figure S4). Ascorbyl radical is an intermediate formed during the oxidation of ascorbic acid by oxygen, and Electron spin resonance (ESR) can directly detect this radical [17]. Thus, the ESR spectra of the ascorbyl radical were measured both at CuPt and AA oxidase (AAO) (Figure 4C). This effect of CuPt on AA was similar to AA oxidase [3,17], indicating CuPt had AA oxidase-like activity. As it is well known, reactive oxygen species (ROS) play a key role in oxidation-reduction reactions. To figure out what kind of ROS play an important role in the effect of CuPt on AA, mannitol (·OH scavenger) and histidine (scavenger of singlet oxygen) [18] were supplemented in the system, which led to the decrease of extinction change of the solution to different degrees. The extinction decreased significantly in the presence of histidine, which suggested the singlet oxygen play a major role in the reaction of AA and CuPt (Figure 4D). These results demonstrated that CuPt can reduce the antioxidant activity of AA.

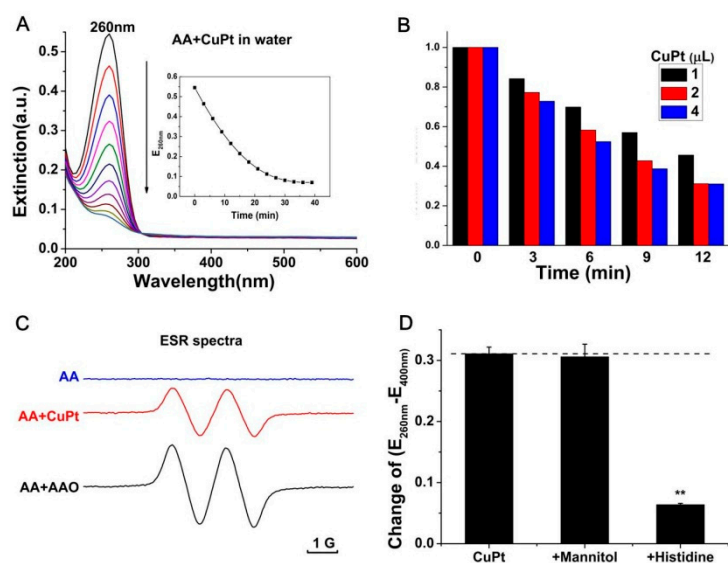


**Figure 4.** Antioxidant assay of AA. **(A)** UV-Vis-NIR spectra of AA after incubation with 1  $\mu$ L CuPt for every 3 min. Insert was the change of extinction at 260 nm with time. **(B)** The extinction changed with different concentrations of AA. **(C)** Electron spin resonance (ESR) spectrum of the ascorbyl radical. [AA] = 50  $\mu$ g/mL, [AAO] = 0.2 U/mL, and the volume of CuPt was 0.005  $\mu$ L. **(D)** The inhibitory effect on the oxidation of AA by incubating with mannitol and histidine for 2 min. The concentrations were [AA] = 57  $\mu$ M, [mannitol] = 5.50 mM, and [histidine] = 6.40 mM, and CuPt = 4  $\mu$ L.

#### 2.4. Antioxidant Activity of AA Detected by DPPH

$\alpha$ ,  $\alpha$ -diphenyl- $\beta$ -picrylhydrazyl (DPPH), is a free radical scavenger to determine the antioxidant activity of a compound [19]. The antioxidant activity of AA in the absence or present of CuPt was investigated with the extinction spectra. Both the extinctions at 520 nm (characteristic absorption peak for DPPH) and 260 nm changed over time (Figure 5A). To evaluate the antioxidant activity of AA after reacted with CuPt, the extinction of mixed solution with different concentrations of CuPt was monitored. The extinction at 260 nm decreased, while the one at 520 nm had no obvious changes (Figure 5B,C), which indicated the DPPH method was not adaptive to determinate the antioxidant activity of AA in the presence of CuPt. Note, the change of extinction at 260 nm was more obvious than that at 520 nm, indicating CuPt reduced the ability of AA to scavenge DPPH. This also showed that AA preferred to interact with CuPt instead of DPPH. By adding histidine, the change rate of extinction at 260 nm decreased (Figure 5D). This was consistent with the effect of CuPt on AA, indicating that histidine can inhibit the interaction between CuPt and AA.

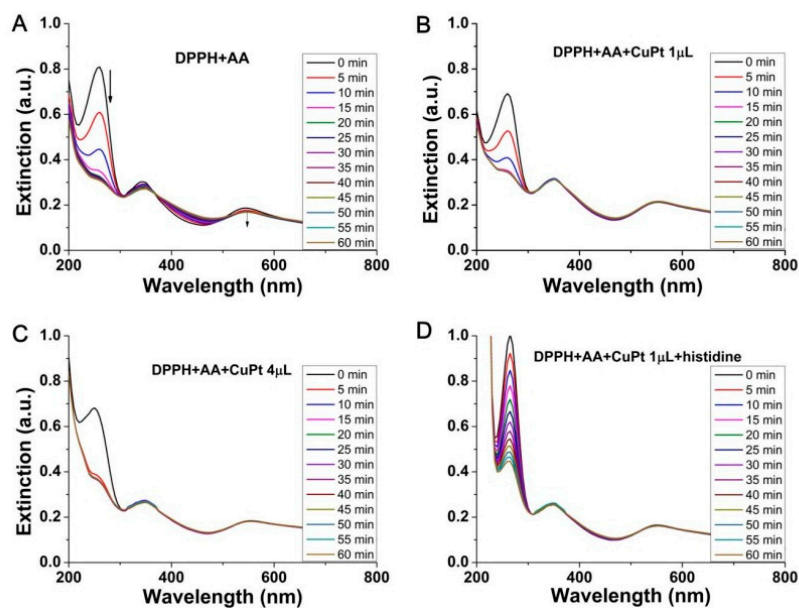


**Figure 5.** Antioxidant capacity of AA measured by  $\alpha$ ,  $\alpha$ -diphenyl- $\beta$ -picrylhydrazyl (DPPH) assay. The concentration-dependent acceleration of CuPt reacted with the mixture containing DPPH and AA measured by every 5 min. The concentrations are [DPPH] = 25  $\mu$ M, [AA] = 57  $\mu$ M, CuPt anocomposite were 0  $\mu$ L for (A), 1  $\mu$ L for (B) and (D), 4  $\mu$ L for (C), [histidine] = 6.40 mM for (D).

### 2.5. Interaction of CuPt with DPPH

As mentioned in Section 2.4, CuPt interfered with the reaction of AA and DPPH; we further investigated whether CuPt had influences on DPPH in the absence of AA. The extinction of DPPH changed in the presence of CuPt, showing CuPt interacted with DPPH alone (Figure 6A). This reaction was also in a concentration dependent manner (Figure 6B and Figure S5). In the presence of histidine, the extinction changes were inhibited significantly (Figure 6B and Figure S5). A LED light source with full wavelength was used to irradiate the solution of CuPt and DPPH. The temperature of solution reached no more than 30 °C after irradiating 5 min (Figure S6) using thermoelectric pair. It was found that the extinction of DPPH changed more after the irradiation than that without light irradiation or the solution at 30 °C in the presence of CuPt (Figure 6C), showing the photocatalysis effect on DPPH in the presence of CuPt. To rule out the influence of light on DPPH itself, the extinction change of DPPH solutions was investigated in the absence or presence of CuPt. As shown in Figure 6D, the extinction of solutions containing DPPH and being irradiated by light changed more in the presence of CuPt than that in the absence of CuPt. As DPPH is a stable radical and the signal attenuation of DPPH is one of the criteria widely used to demonstrate the ability to scavenge ROS [20], and this result showed the quenching effect of CuPt on DPPH both in the absence or present of light, therefore, the photocatalytic effect of CuPt on DPPH required much attention to be paid in the application of DPPH.

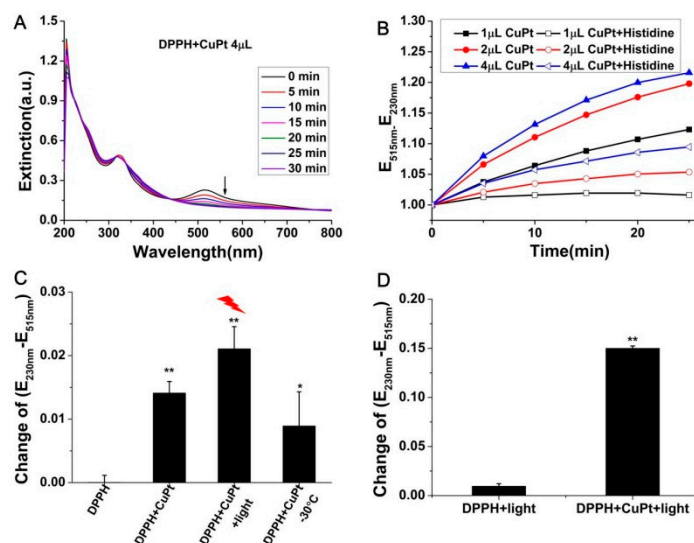


**Figure 6.** DPPH scavenging capacity and the photo-enhanced activity of CuPt. (A) UV-Vis-NIR spectra of DPPH after incubation with 4 μL CuPt for 30 min at the time interval of 5 min. (B) The extinction changes and the inhibition effect of histidine for DPPH in different concentration of CuPt. (C) The photo-enhanced oxidation of DPPH with 1 μL CuPt after 5 min. The temperature was 30 °C under the light after 5 min. (D) The photo-enhanced oxidation of DPPH with 4 μL CuPt after 15 min. The concentrations were [DPPH] = 25 μM, [histidine] = 6.40 mM for (A), (B), (C) and (D).

According to the literature, Pt-based nanoparticle has excellent properties with POD-like activity [21], AAO-like activity [22], scavenge DPPH [23], and photocatalytic effect [24]. Incorporation of metals resulted in the change of electronic structure of Pt, and it is an effective way to improve catalytic and photocatalytic activity [24,25]. The catalytic and photocatalytic activity of Pt-based NPs mainly resulted from the production of ROS and light-induced electron–hole separation [26], and the mechanism of CuPt might be similar.

### 3. Materials and Methods

#### 3.1. Materials

Potassium tetrachloroplatinate (II) ( $K_2PtCl_4$ ), poly(styrenesulfate) (PSS), histidine, ascorbic acid (AA), and mannitol were all purchased from Alfa Aesar. Horseradish peroxidase (HRP) and ascorbate oxidase (AAO) were purchased from Sigma Aldrich (St. Louis, MO, USA). Hydrogen peroxide ( $H_2O_2$ , 30 %) was purchased from Beijing Shiji (Beijing, China). Copper sulphate ( $CuSO_4$ ),  $\alpha$ ,  $\alpha$ -diphenyl- $\beta$ -picrylhydrazyl (DPPH) was purchased from Shanghai Macklin Biochemical Co., Ltd. (Shanghai, China). O-Phenylenediamine (OPD) was purchased from Aladdin Co., Ltd. (Shanghai, China). All the reagents were used as received. Milli-Q water (18 M $\Omega$  cm) was used for preparation of all solutions.

#### 3.2. Preparation of CuPt

With 1.2 mM  $CuSO_4$  and 0.4 mM  $K_2PtCl_4$  in the solution containing 0.05 mg mL<sup>-1</sup> PSS (containing 3 mM NaCl), AA (160 mM) was added to co-reduction  $Cu^{2+}$  and  $Pt^{2+}$ . The mixed solution was incubated in the water bath (30 °C) for 2 h. The suspension was centrifuged once (12000 rpm 5 min) and the precipitate was dispersed in 100 μL  $H_2O$ , and then used directly in experiments.

#### 3.3. Characterization

Scanning electron microscopy (SEM) images were taken on a field emission scanning electron microscope (FESEM, Hitachi S-4800, Tokyo, Japan). Transmission electron microscopy (TEM) images

were captured at an accelerating voltage of 200 kV from TEM-1400 plus microscope (JEOL, Tokyo, Japan). Elemental analysis was performed with energy-dispersive X-ray (EDX) from SEM. X-ray diffraction (XRD) was performed with Bruker D8 Advance powder X-ray diffractometer (Billerica, MA, USA). All UV-Vis-NIR spectral data were collected from suspensions in cuvettes and were conducted on a Lambda 950 ultraviolet-visible-near infrared (UV-Vis-NIR) spectrometer (PerkinElmer Co., Ltd., Waltham, MA, USA).

#### 3.4. Peroxidase (POD)-like Activity of CuPt

The peroxidase-like property of CuPt was investigated using  $H_2O_2$  and OPD as substrates. Phosphate buffer solution (PBS) as the solvent which contains 2 mM  $KH_2PO_4$ , 8 mM  $Na_2HPO_4$ , 136 mM NaCl, 2.6 mM KCl. Mixture of 2.0 mL PBS, 100  $\mu$ L  $H_2O_2$  (10 M), 10  $\mu$ L OPD (0.92 M), were added in a quartz colorimetric pool in the absence or presence of 1  $\mu$ L CuPt solution. The pH dependence analysis was conducted using PBS with pH ranging from 2 to 10 adjusted with HCl (12 M) or NaOH (1 M). The concentration-dependent absorbance changes of CuPt were consecutively recorded at 450 nm.

#### 3.5. $H_2O_2$ Detection

For detection of  $H_2O_2$ , 1  $\mu$ L CuPt solution was added into 2.0 mL water, containing 100  $\mu$ L  $H_2O_2$  with different concentrations (0–50  $\mu$ M), and 10  $\mu$ L OPD solution (0.92 M). The mixture was subjected to room temperature for 10 min. Then the absorbance at 450 nm was recorded by using the Synergy H1 Hybrid Multi-Mode microplate reader (BioTek Instruments, Winooski, VT, USA).

#### 3.6. Effect of CuPt on AA

The oxidation of AA was also detected by a spectrophotometric method. Mixture of 2.0 mL ascorbic acid (AA, 57  $\mu$ M) and CuPt solution with different volumes (1–4  $\mu$ L) were added. Then the absorbance at 260 nm was recorded. Electron spin resonance (ESR) technique was employed to investigate the activity of AAO and CuPt on AA. ESR measurements were performed with a Bruker EMX ESR spectrometer (Billerica, MA, USA) at ambient temperature. Specifically, aliquots of approximately 50  $\mu$ L of samples were pipetted into glass capillary tubes with 1 mm internal diameter and sealed. The spectra of the capillary tubes were recorded at 4 min. Other settings included 30 G scan range and 1 G field modulation, 20 mW microwave power for detection of AA radical.

#### 3.7. Antioxidant Activity of AA Detected by DPPH

The antioxidation activity of AA measured by DPPH method was examined. The experimental system contains different volume (1 and 4  $\mu$ L) CuPt solution, 2  $\mu$ L AA (57 mM), and 2.0 mL DPPH (25  $\mu$ M).

#### 3.8. Interaction of CuPt with DPPH

Free radical scavenging activities of CuPt were measured by the mixture of 2.0 mL DPPH solution (25  $\mu$ M) and CuPt with different volumes (1–4  $\mu$ L).

#### 3.9. The Photo-Enhanced Activity on DPPH

The photo-enhanced activities for the DPPH scavenging capacity of CuPt were detected as the above method. The light source was a LED with the power of 15 W. The temperature was recorded during the light by a thermoelectric pair. And the experiment was repeated without light in the water bath at the same temperature for the same time to avoid the effect of temperature caused by light.

To examine the possible radicals in experiment system, 20  $\mu$ L histidine (0.64 M) and 10  $\mu$ L mannitol (1.10 M) were added to the mixed solutions.

### 3.10. Statistical Analysis

The experiments were performed three times and presented as mean values  $\pm$  standard deviation. Statistical significances were analyzed using the Student's t-test and ANOVA.  $P < 0.05$ , \*;  $P < 0.01$ , \*\*.

## 4. Conclusions

In summary, the CuPt with diameter ca. 125 nm were synthesized with a simply co-reduction method. This CuPt showed a POD-like activity on the substrate of OPD and AAO-like activity by investigating their UV-vis-NIR spectra. CuPt was found to interfere with the reaction between AA and DPPH when using DPPH method to determinate the antioxidant activity of AA. In the presence of light, the reaction between DPPH and CuPt were enhanced, which indicates a photocatalysis role of CuPt on DPPH. With adding histidine, the AA oxidase-like activity and effects on DPPH were inhibited. We hope the findings here benefit the research on the properties and applications of nanocomposites.

**Supplementary Materials:** The following are available online at <http://www.mdpi.com/2073-4344/9/10/813/s1>, Figure S1: Characterizations of the nanocomposite consisting of Cu and Pt (CuPt), Figure S2: Extinction spectra of OPD in the presence of 1  $\mu$ L CuPt in PBS with different pH, Figure S3: Extinction spectra of OPD with different concentrations of CuPt in PBS (pH = 3.65), Figure S4: Extinction spectra of AA with different concentrations of CuPt, Figure S5: UV-Vis-NIR spectra of DPPH after incubation with different concentration of CuPt without and with histidine. Figure S6: Temperature curve of solution containing DPPH and 1  $\mu$ L CuPt.

**Author Contributions:** All authors contributed to data analysis, drafting or revising the article, gave final approval of the version to be published, and agree to be accountable for all aspects of the work.

**Funding:** This work was supported by the National Key R&D Program of China (2017YFA0205504), National Natural Science Foundation of China (81801771), and CAMS Innovation Fund for Medical Sciences (CIFMS 2016-I2M-3-004 and 2018-I2M-3-006).

**Acknowledgments:** We would like to thank Jun-Jie Yin (Center for Food Safety and Applied Nutrition, U.S. Food and Drug Administration) for his help on the experiments involved radical.

**Conflicts of Interest:** The authors declare no conflict of interest.

## References

1. Wang, J.; Gu, H. Novel Metal Nanomaterials and Their Catalytic Applications. *Molecules* **2015**, *20*, 17070–17092. [[CrossRef](#)] [[PubMed](#)]
2. Wei, H.; Wang, E. Nanomaterials with enzyme-like characteristics (nanozymes): Next-generation artificial enzymes. *Chem. Soc. Rev.* **2013**, *42*, 6060–6093. [[CrossRef](#)] [[PubMed](#)]
3. Wang, Y.; Yang, Y.; Liu, W.; Ding, F.; Zou, P.; Wang, X.; Zhao, Q.; Rao, H. A carbon dot-based ratiometric fluorometric and colorimetric method for determination of ascorbic acid and of the activity of ascorbic acid oxidase. *Microchim. Acta* **2019**, *186*, 246. [[CrossRef](#)] [[PubMed](#)]
4. Jiang, D.; Ni, D.; Rosenkrans, Z.T.; Huang, P.; Yan, X.; Cai, W. Nanozyme: New horizons for responsive biomedical applications. *Chem. Soc. Rev.* **2019**, *48*, 3683–3704. [[CrossRef](#)] [[PubMed](#)]
5. Guo, X.; Zhang, Y.; Deng, C.; Li, X.; Xue, Y.; Yan, Y.M.; Sun, K. Composition dependent activity of Cu-Pt nanocrystals for electrochemical reduction of CO<sub>2</sub>. *Chem. Commun.* **2015**, *51*, 1345–1348. [[CrossRef](#)]
6. Dobrucka, R.; Dlugaszewska, J. Antimicrobial activity of the biogenically synthesized core-shell Cu@Pt nanoparticles. *Saudi Pharm. J.* **2018**, *26*, 643–650. [[CrossRef](#)] [[PubMed](#)]
7. Shiraishi, Y.; Sakamoto, H.; Sugano, Y.; Ichikawa, S.; Hirai, T. Pt-Cu Bimetallic Alloy Nanoparticles Supported on Anatase TiO<sub>2</sub>: Highly Active Catalysts for Aerobic Oxidation Driven by Visible Light. *ACS Nano* **2013**, *7*, 9287–9297. [[CrossRef](#)]
8. Nosheen, F.; Ni, B.; Xu, X.; Yang, H.; Zhang, Z.; Wang, X. Facile synthesis of complex shaped Pt-Cu alloy architectures. *Nanoscale* **2016**, *8*, 13212–13216. [[CrossRef](#)]
9. Lu, Y.; Ye, W.; Yang, Q.; Yu, J.; Wang, Q.; Zhou, P.; Wang, C.; Xue, D.; Zhao, S. Three-dimensional hierarchical porous PtCu dendrites: A highly efficient peroxidase nanozyme for colorimetric detection of H<sub>2</sub>O<sub>2</sub>. *Sens. Actuators B Chem.* **2016**, *230*, 721–730. [[CrossRef](#)]

10. Lian, Q.; Liu, H.; Zheng, X.; Li, X.; Zhang, F.; Gao, J. Enhanced peroxidase-like activity of CuO/Pt nanoflowers for colorimetric and ultrasensitive Hg<sup>2+</sup> detection in water sample. *Appl. Surf. Sci.* **2019**, *483*, 551–561. [[CrossRef](#)]
11. Zhang, X.; Jiang, X.; Croley, T.R.; Boudreau, M.D.; He, W.; Cai, J.; Li, P.; Yin, J.J. Ferroxidase-like and antibacterial activity of PtCu alloy nanoparticles. *J. Environ. Sci. Health Part C Environ. Carcinog. Ecotoxicol. Rev.* **2019**, *37*, 99–115. [[CrossRef](#)] [[PubMed](#)]
12. Xu, D.; Liu, Z.; Yang, H.; Liu, Q.; Zhang, J.; Fang, J.; Zou, S.; Sun, K. Solution-based evolution and enhanced methanol oxidation activity of monodisperse platinum-copper nanocubes. *Angew. Chem. Int. Ed. Engl.* **2009**, *48*, 4217–4221. [[CrossRef](#)] [[PubMed](#)]
13. Liu, Q.; Yan, Z.; Henderson, N.L.; Bauer, J.C.; Goodman, D.W.; Batteas, J.D.; Schaak, R.E. Synthesis of CuPt Nanorod Catalysts with Tunable Lengths. *J. Am. Chem. Soc.* **2009**, *131*, 5720–5721. [[CrossRef](#)] [[PubMed](#)]
14. Wu, J.; Wang, X.; Wang, Q.; Lou, Z.; Li, S.; Zhu, Y.; Qin, L.; Wei, H. Nanomaterials with enzyme-like characteristics (nanozymes): Next-generation artificial enzymes (II). *Chem. Soc. Rev.* **2018**, *48*, 1004–1079. [[CrossRef](#)] [[PubMed](#)]
15. Jiang, B.; Duan, D.; Gao, L.; Zhou, M.; Fan, K.; Tang, Y.; Xi, J.; Bi, Y.; Tong, Z.; Gao, G.F.; et al. Standardized assays for determining the catalytic activity and kinetics of peroxidase-like nanozymes. *Nat. Protoc.* **2018**, *13*, 1506–1520. [[CrossRef](#)] [[PubMed](#)]
16. Hempen, C.; van Leeuwen, S.M.; Luftmann, H.; Karst, U. Liquid chromatographic/mass spectrometric investigation on the reaction products in the peroxidase-catalyzed oxidation of o-phenylenediamine by hydrogen peroxide. *Anal. Bioanal. Chem.* **2005**, *382*, 234–238. [[CrossRef](#)] [[PubMed](#)]
17. Zhou, Y.T.; He, W.; Wamer, W.G.; Hu, X.; Wu, X.; Lo, Y.M.; Yin, J.J. Enzyme-mimetic effects of gold@platinum nanorods on the antioxidant activity of ascorbic acid. *Nanoscale* **2013**, *5*, 1583–1591. [[CrossRef](#)]
18. Gao, L.; Liu, R.; Gao, F.; Wang, Y.; Jiang, X.; Gao, X. Plasmon-Mediated Generation of Reactive Oxygen Species from Near-Infrared Light Excited Gold Nanocages for Photodynamic Therapy in Vitro. *ACS Nano* **2014**, *8*, 7260–7271. [[CrossRef](#)]
19. Kedare, S.B.; Singh, R.P. Genesis and development of DPPH method of antioxidant assay. *J. Food Sci. Technol.* **2011**, *48*, 412–422. [[CrossRef](#)]
20. Jing, P.; Zhao, S.J.; Jian, W.J.; Qian, B.J.; Dong, Y.; Pang, J. Quantitative studies on structure-DPPH\* scavenging activity relationships of food phenolic acids. *Molecules* **2012**, *17*, 12910–12924. [[CrossRef](#)]
21. Liu, Y.; Wu, H.; Li, M.; Yin, J.-J.; Nie, Z. pH dependent catalytic activities of platinum nanoparticles with respect to the decomposition of hydrogen peroxide and scavenging of superoxide and singlet oxygen. *Nanoscale* **2014**, *6*, 11904–11910. [[CrossRef](#)] [[PubMed](#)]
22. Chen, C.; Fan, S.; Li, C.; Chong, Y.; Tian, X.; Zheng, J.; Fu, P.P.; Jiang, X.; Wamer, W.G.; Yin, J.-J. Platinum nanoparticles inhibit antioxidant effects of vitamin C via ascorbate oxidase-mimetic activity. *J. Mater. Chem. B* **2016**, *4*, 7895–7901. [[CrossRef](#)]
23. Watanabe, A.; Kajita, M.; Kim, J.; Kanayama, A.; Takahashi, K.; Mashino, T.; Miyamoto, Y. In vitro free radical scavenging activity of platinum nanoparticles. *Nanotechnology* **2009**, *20*, 455105. [[CrossRef](#)] [[PubMed](#)]
24. Zhang, L.; Jia, H.; Liu, C.; Liu, M.; Meng, Q.; He, W. Enhanced generation of reactive oxygen species and photocatalytic activity by Pt-based metallic nanostructures: The composition matters. *J. Environ. Sci. Health Part C Environ. Carcinog. Ecotoxicol. Rev.* **2019**, *37*, 1–13. [[CrossRef](#)] [[PubMed](#)]
25. He, W.; Kim, H.K.; Wamer, W.G.; Melka, D.; Callahan, J.H.; Yin, J.J. Photogenerated charge carriers and reactive oxygen species in ZnO/Au hybrid nanostructures with enhanced photocatalytic and antibacterial activity. *J. Am. Chem. Soc.* **2014**, *136*, 750–757. [[CrossRef](#)] [[PubMed](#)]
26. Jiang, X.; He, W.; Zhang, X.; Wu, Y.; Zhang, Q.; Cao, G.; Zhang, H.; Zheng, J.; Croley, T.R.; Yin, J.-J. Light-Induced Assembly of Metal Nanoparticles on ZnO Enhances the Generation of Charge Carriers, Reactive Oxygen Species and Antibacterial Activity. *J. Phys. Chem. C* **2018**, *122*, 29414–29425. [[CrossRef](#)]

